Fundamental Limits of Disk Flexure Resonators

Jonathan M. Puder
OxideMEMS Lab
Cornell University
Ithaca, USA

Jeffrey S. Pulskamp, Ryan Q. Rudy, and Ronald G. Polcawich
Sensors and Electron Devices Directorate
US Army Research Laboratory
Adelphi, USA

Sunil A. Bhave
OxideMEMS Lab
Purdue University
West Lafayette, IN

***Abstract*— High performance PZT-on-silicon disk flexure resonators were recently demonstrated with peak |S21| of -1 dB with direct 50 Ω termination, high bandwidth tunability, and high coupling at 22 MHz. This paper explores the performance limits and design optimization of this new resonator in the space of radius and silicon thickness of the (1,1) disk flexure mode. This effort is enabled by the Rapid Analytical/FEA Technique, a novel method for expedited acoustic resonator simulation. Simulations indicate that monolithic integration of disk resonators with -0.5 dB max|S21| may be achieved across a wide range of HF and low-VHF frequencies without the need for external impedance matching.**

Keywords—component; formatting; style; styling; insert (key words)

I. Introduction

Piezoelectric MEMS contour resonators and filters promise frequency agility in an increasingly crowded and dynamic electromagnetic environment. The center frequencies of these devices are lithographically defined, enabling the monolithic integration of filter banks on a single chip. While recent research has focused on commercial interests in the UHF to S bands, military applications still demand high performance devices below 500 MHz.

Recently a PZT-on-silicon [1,2,3,4] device consisting of six electrically parallel disk flexure resonators (DFR) terminated directly to 50 Ω demonstrated a peak $|S_{21}|$ of -1 dB at 22 MHz, and insertion loss, *IL*, of 0.92 dB [5]. The motional resistance, R_m, was 9 Ω, and high electromechanical coupling (k_{eff}^2) and bandwidth tuning were demonstrated. To understand if this performance may be realized at higher frequencies, this paper investigates the fundamental performance and frequency limits of piezoelectric-on-silicon DFRs supported by the novel Rapid Analytical/FEA Technique (RAFT) [6]. This modeling technique enables designers to accurately simulate the scattering (S) parameters of piezoelectrically transduced resonators with full 3D models orders of magnitude faster than commercially available FEA packages. With the help of the RAFT, the results of a parametric study of the scaling of R_m, max $|S_{21}|$, k_{eff}^2, f_r, and figure of merit (*FOM*) with disk radius (r_{disk}) and the silicon thickness (t_{Si}) are presented.

II. Ease of Use

The RAFT requires the same parameters (moduli, density, piezoelectric coefficients, etc.) as standard FEA. To address the fact that mechanical quality factor is often not known before

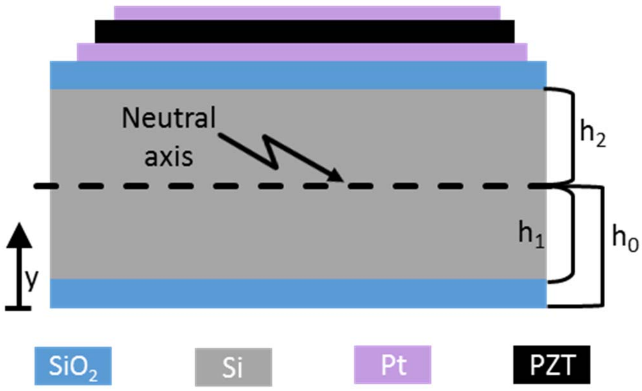

Fig. 1. A schematic of the PZT on silicon resonator with the definition of y and h_n denoted.

fabrication and testing, a "volumetric" material quality factor (Q_{mat}) was derived dependent on material loss, thickness, and stress profile and is given by

$$Q_{mat} = \frac{Y_1\, y^3|_{h_0}^{h_1} + Y_2\, y^3|_{h_1}^{h_2} + \cdots + Y_n\, y^3|_{h_{n-1}}^{h_n}}{\frac{Y_1}{Q_1}\, y^3|_{h_0}^{h_1} + \frac{Y_1}{Q_2}\, y^3|_{h_1}^{h_2} + \cdots + \frac{Y_n}{Q_n}\, y^3|_{h_{n-1}}^{h_n}} \quad (1)$$

Where Y is the elastic modulus, y is the distance from the neutral axis, h is the distance of the top of the n^{th} layer from the neutral axis, and Q_n is the material quality factor of the n^{th} layer. A schematic of the geometric parameters for a PZT on silicon stack may be seen in Fig 1. Assigned material quality factors for silicon dioxide, silicon, platinum and PZT in that order were: 100, 100,000, 100, and 200. In addition, a "limiting" Q_{lim} of 750 was added to the resonator to avoid abnormally high Q_m.

$$Q_m = \frac{Q_{mat} \cdot Q_{lim}}{Q_{mat} + Q_{lim}} \quad (2)$$

For accurate and realistic simulation, required parameters were measured, extracted from test structures, or taken from design. The elastic moduli of the material stack were independently measured [7], and densities were taken from bulk measurements. Piezoelectric coefficients were set to 10 C/m^2, a value within the range extracted from on-wafer cantilever test structures. Tether resistances were derived from designed dimensions and resistivity test structures, and permittivity was extracted from fabricated devices. Lateral dimensions for model

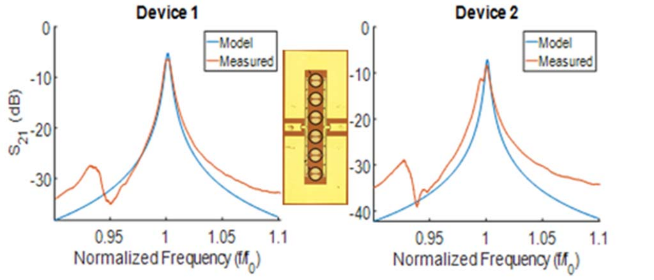

Fig. 2. Agreement between model and experiment. Fabricated devices consist of six 77 MHz resonators in parallel. Sources of discrepancy are nearby spurious modes and frequency misalignment of individual resonators. See inset for image of fabricated resonators.

validation were taken from design, and layer thicknesses were taken from nominal deposition thicknesses.

To parametrically explore the design space of DFRs, 250 simulations to generate S parameters were run at various r_{disk} and t_{Si} for a total simulation time of 27 hours, or 6.5 minutes per simulation. This low simulation time was enabled by the RAFT, in which rapid Eigen frequency simulations are run first. These are then processed in an analytical software package utilizing a generalized expression for R_m. r_{disk} varied from 12 to 60 µm, and t_{Si} varied from 1 to 10 µm.

III. Results

A. Validation

The model was validated against measurements of devices consisting of six electrically parallel DFRs using measured Q_m and extracted on-wafer e_{31} (Fig. 2). Since this paper is only concerned with the (1,1) disk flexure mode, spurious modes were not modeled in these measurements, and are the largest source of discrepancy.

B. Simulation Results

Contour plots of the performance parameters extracted from the simulations versus t_{Si} and r_{disk} may be seen in Figs. 3, 4, 5 and 5. The performance of the device from [5] is marked by a star in these figures Figs. 3-6. Fig. 3, 4, and 5 indicate that max|S_{21}|, R_m, k_{eff}^2, and *FOM* are all primarily determined by the t_{Si}, and nearly constant across r_{disk}. This agrees with the result from [8], in which an analytical expression for the R_m of the (1,1) mode of disk flexure is presented. Given this, devices with similar performance parameters may be designed across a wide range of frequencies by adjusting r_{disk} (Fig 6). Fig. 3 and 4a indicate that for single resonators, the lowest R_m and max|S_{21}| that may be obtained are at higher t_{Si}. However, when disks are placed electrically in parallel to obtain approximately 50 Ω shunt reactance, the lowest loss of ~0.5 dB occurs at ~2.5 µm t_{Si} across all r_{disk} (Fig. 4b). This region coincides with the region of optimal *FOM* in Fig. 5b. This result stems from properties of the PZT-on-silicon stack and flexure based resonators. By adding silicon, a high Q_m material, to PZT, a low Q_m material, the resonator coupling is reduced, while the overall resonator Q_m. increases. At zero t_{Si}, there should be no coupling since the neutral axis would coincide with the mid-plane of the piezoelectric layer, and no bending moment would exist. At large t_{Si}, most of resonator would be a non-piezoelectric, and coupling would be minimized. Therefore, there must be an optimal t_{Si} for maximized *FOM*, which simulations suggest are ~2.5 µm and 35, respectively, with a Q_m of 580.

The upper frequency limit for high performance disks occurs around 100 MHz. At this frequencies, the r_{disk} is less than 2.5 times t_{Si}. The mode transforms and begins to store more energy in in-plane shear, which is not directly transduced by PZT. The effects of this may be seen in the upper left hand corner of Fig. 3, 4, and 5, where the performance metrics sharply dip. A comparison of the displacements of a mode with favorable and unfavorable r_{disk}/t_{Si} is shown in Fig 7.

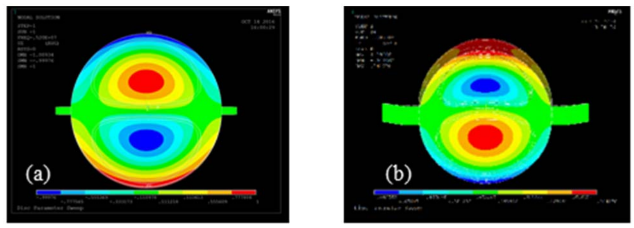

Fig. 7. Top view of simulated disks' out of plane displacement. (a) has a favorable r_{disk}/t_{Si} ratio, while (b) exhibit high shear, noticeable along the top edge, which creates a significant displacement of the anchors.

C. Comparison to -1 dB Device

The RAFT accurately predicted the performance of the device from [5] despite using a nominal e_{31} of 10 C/m^2 and an

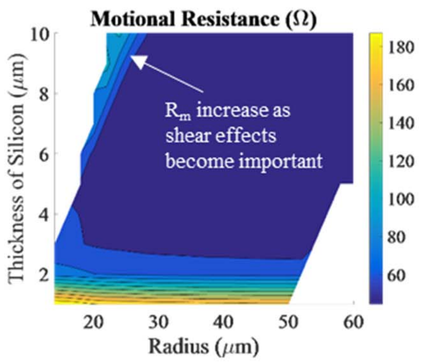

Fig. 3. Modeled R_m of a single resonator as a function of r_{disk} and t_{Si}. Note at r_{disk}/t_{Si} and as r_{disk} approaches t_{Si}, R_m begins to increase.

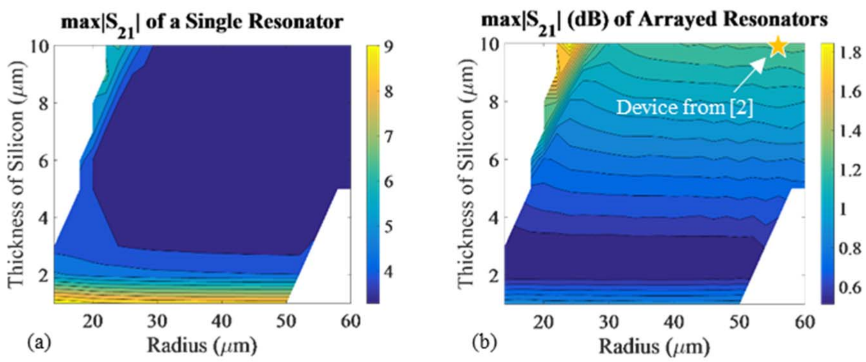

Fig. 4. Maximum |S_{21}| for (a) a single resonator (b) resonators cascaded for 50 Ω shunt impedance. Note loss increasing with low r_{disk}/t_{Si} ratios. Optimal designs are predicted to have loss ~ -0.5 dB.

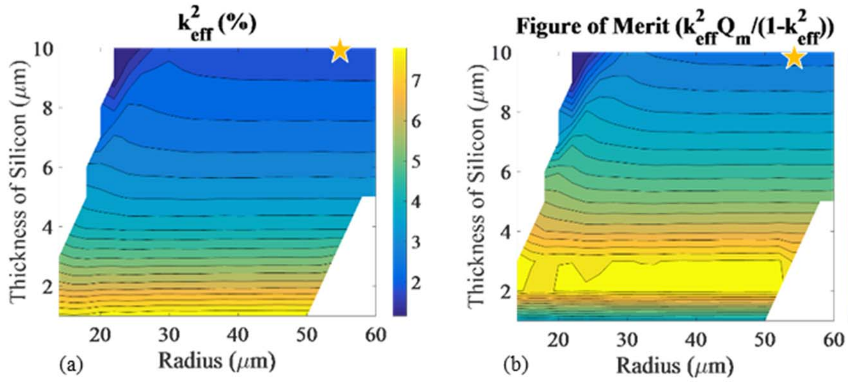

Fig. 5. The (a) electromechanical coupling and (b) Figure of Merit (*FOM*) predicted. Ratios of shunt and motional capacitances were used to arrive at k_{eff}^2 and volumetric Q_m was used to arrive at the *FOM*.

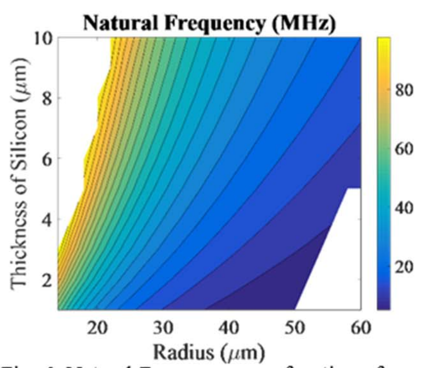

Fig. 6. Natural Frequency as a function of r_{disk} and t_{Si}. Limiting frequencies are near 100 MHz before shear starts to degrade the mode.

analytically modeled Q_m, with an included limiting Q, to predict R_m. The relative permittivity was also set to a typical value of 440. Resonator performance parameters for the simulated and fabricated device may be seen in Table 1. This shows that the RAFT can effectively predict the performance of low loss devices, even without properties extracted from test structures.

TABLE I. COMPARISON OF SIMULATION AND MEASUREMENT

	Fabricated Device	*Simulated Device*
Maximum S_{21} (dB)	-1	-1.28
k_{eff}^2(%)	2.09	1.95
Q_m	815	741
Figure of Merit ($k_{eff}^2 \cdot Q_m$)	16.9	14.73
R_m (Ω)	9	7.5

IV. CONCLUSION

Monolithically integrated disk resonators terminated directly to 50 Ω have been predicted to have low losses of -0.5 dB max|S_{21}| across a wide range of frequencies when placed in parallel electrically. The model, which used typical values for material properties and Q_m, was compared to the fabricated -1 dB device and was able to accurately predict performance parameters. The upper limit for sub-1 dB loss occurs around 90 MHz, when the mode beings to store more energy in in-plane shear. The model also predicts a point of maximum *FOM*, which coincides with optimal max|S_{21}|, where added silicon enhances Q_m more than it decreases k_{eff}^2. These results suggest that general out-of-plane flexure devices have potential to be high performance devices at low frequencies.

[1] Pulskamp, J.S., et. al. (2012). "Electrode-shaping for the excitation and detection of permitted arbitrary modes in arbitrary geometries in piezoelectric resonators." *IEEE Trans. Ultrason., Ferroelect., Freq. Cont.*

[2] S. S. Bedair, J. S. Pulskamp, R. G. Polcawich, R. Q. Rudy and J. Puder, "Thin-film piezoelectric transformers operating in harmonics of out-of-plane flexure modes," *2015 Transducers - 2015 18th International Conference on Solid-State Sensors, Actuators and Microsystems (TRANSDUCERS)*, Anchorage, AK, 2015, pp. 714-717.

[3] J. S. Pulskamp, R. Q. Rudy, S. S. Bedair, J. M. Puder, M. G. Breen and R. G. Polcawich, "Ferroelectric PZT MEMS HF/VHF resonators/filters," *2016 IEEE International Frequency Control Symposium (IFCS)*, New Orleans, LA, 2016, pp. 1-4.

[4] J. S. Pulskamp, S. S. Bedair, G. Ronald and S. A. Bhave, "Ferroelectric PZT RF MEMS resonators," *2011 Joint Conference of the IEEE International Frequency Control and the European Frequency and Time Forum (FCS) Proceedings*, San Fransisco, CA, 2011, pp. 1-6.

[5] Rudy, R.Q, et al.(2016). "Piezoelectric Disk Flexure Resonator with 1 dB Loss." *2016 Proc. IEEE Intl. Freq. Cont. Symp*.

[6] Puder, J.M.. et al. "Orders of Magnitude Reduction in Acoustic Resonator Simulation Times via the Wide-Band Rapid Analytical-FEA Technique." *2017 IEEE Intl. Fre. Cont. Symp*, accepted.

[7] Yagnamurthy, S., et. al. (2011). "Mechanical and Ferroelectric Behavior of PZT-Based Thin Films." *J. of Microelectromech Syst.*, vol. 20, no. 6.

[8] Puder, J.M.. et al. "Analytical Modeling of Low Loss Disk Flexure Resonators." *2017 IEEE Intl. Fre. Cont. Symp*, accepted.